Applied Energy 306 (2022) 118092

Contents lists available at ScienceDirect

Applied Energy

journal homepage: www.elsevier.com/locate/apenergy

Resilience-oriented schedule of microgrids with hybrid energy storage system using model predictive control

Javier Tobajas [a,*], Felix Garcia-Torres [a], Pedro Roncero-Sánchez [c], Javier Vázquez [c], Ladjel Bellatreche [d], Emilio Nieto [b]

[a] Applications Unit, Centro Nacional del Hidrogeno CNH2, Puertollano, Ciudad Real, 13500, Spain
[b] Centro Nacional del Hidrogeno CNH2, Puertollano, Ciudad Real, 13500, Spain
[c] Institute of Energy Research and Industrial Applications, University of Castilla-La Mancha, Ciudad Real, Campus Universitario s/n 13071, Spain
[d] LIAS/ISAE-ENSMA, Poitiers, 86961, France

GRAPHICAL ABSTRACT

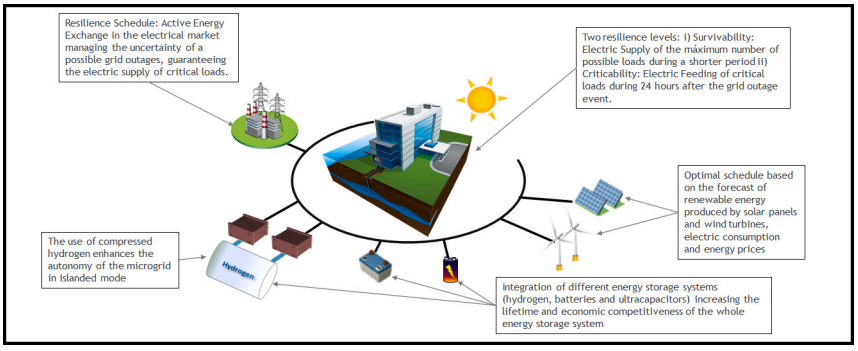

ARTICLE INFO

Keywords:
Energy management
Multi-scenario
MPC
Resilience
Microgrid
Hybrid energy storage system

ABSTRACT

Microgrids can be regarded as a promising solution by which to increase the resilience of power systems in an energy paradigm based on renewable generation. Their main advantage is their ability to work as islanded systems under power grid outage conditions. Microgrids are usually integrated into electrical markets whose schedules are carried out according to economic aspects, while resilience criteria are ignored. This paper shows the development of a resilience-oriented optimization for microgrids with hybrid Energy Storage System (ESS), which is validated via numerical simulations. A hybrid ESS composed of hydrogen and batteries is, therefore, considered with the objective of improving the autonomy of the microgrid while achieving a rapid transition response. The control problem is formulated using Stochastic Model Predictive Control (SMPC) techniques in order to take into account possible transitions between grid-connected and islanded modes at all the sample instants of the schedule horizon (SH). The control problem is developed by considering a healthy operation of the hybrid ESS, thus avoiding degradation issues. The plant is modeled using the Mixed Logic Dynamic (MLD) framework, owing to the presence of logic and dynamic control variables.

1. Introduction

Resilience has, in recent years, become a relevant issue of power systems. One of the reasons for this is the effects that natural disasters may have on electrical grids. The growing concern related to attacks on the cyber and physical assets associated with power grids is another issue to be addressed. In traditional power systems, power quality

* Corresponding author.
E-mail address: javier.tobajas@cnh2.es (J. Tobajas).

https://doi.org/10.1016/j.apenergy.2021.118092
Received 19 April 2021; Received in revised form 21 September 2021; Accepted 17 October 2021
Available online 8 November 2021

Nomenclature

C	Capacity (Wh)
CC	Capital Cost (€)
Cost	Hourly economic Cost (€/h)
Cycles	Number of life cycles
Hours	Number of life hours
J	Cost Function
LOH	Level of Hydrogen (N m^3)
m	Minimum possible value on the control platform
M	Maximum possible value on the control platform
P	Electrical power (W)
SOC	State of Charge (p.u)
T_s	Sample Period
z	Electrical power formulated as MLD variable (W)
δ	on/off state
η	Efficiency (p.u)
χ	Logical degradation state
ϑ	MLD power variation in degradation state (W)
σ	Logical variable start up state
Γ	Energy price (€)

Subscripts

bat	Battery
ch	Charge
cri	Critical
cur	Curtailment
$degr$	Degradation
dis	Discharge
elz	Electrolyzer
fc	Fuel Cell
gen	Generation
$grid$	Main grid
$load$	Load
pur	Purchase of energy
pv	Photovoltaic system
rem	Remaining power
$sale$	Sale of energy
wt	Wind turbine

in a node of the grid is associated with the short circuit power at that point of the grid. Under constant emission, a greater amount of short circuit power results in better voltage quality. The controllability of fossil-fuel power plants on which the centralized generation has been based to date, along with the traditional linear loads, merely cause low level power quality anomalies in comparison with short circuit power in the upstream network [1]. But this scenario will be substantially modified in future decades with the expected penetration ratio of electricity originating from intermittent production systems based on renewable energy. The reliability of the power supply must be considered as a fundamental aspect in environments with critical loads (i.e., hospitals, military facilities, etc.), and is even more important than the economic optimization of their energy management system (EMS). Microgrids could play a very important role in this challenging framework by improving the resilience of power systems based on renewable generation. Microgrids can provide resilience to this kind of facilities through their capacity to form self-sustainable islanded energy systems [2].

1.1. Literature review

The control problem of microgrids is usually divided into three hierarchical control levels, the upper one of which is concerned with its economic optimization [3] and long-term schedule, while the lower one addresses power quality issues [4]. With regard to microgrid resilience, the tertiary control level has to provide sufficient energy autonomy to feed critical and non-critical loads under possible power outage conditions, while the primary and secondary control levels have to guarantee a rapid transition between grid-connected and islanded mode [4]. A review of the resilience strategies applied to microgrids can be found in [2,5–7]. Several authors have integrated fault tolerance control methods into the EMSs of microgrids [8–11].

The survivability concept for microgrids is introduced in [12,13]. In [14], an optimal schedule for microgrids is carried out by considering uncertainties in generation, load consumption and possible main grid supply interruptions. A resilience-oriented optimization strategy is proposed in [15], considering feasible islanding under normal operation and the survivability of critical loads during emergency periods. A methodology with which to identify the vulnerable components and ensure resilient operation when considering multiple disruptions within the microgrid is presented in [16]. An economic schedule of microgrids with ESS for their participation in the electrical market is carried out in [17], in which the lower bounds of the ESS capacity are reserved as a resilience mechanism. In [18], the methodology outlined in [17] is enhanced to include energy forecast uncertainties using a stochastic formulation of MPC. In [19], a real-time control based on MPC techniques is proposed following a specific schedule of the microgrid.

The authors of [20] develop an innovative fault tolerant consensus-based secondary voltage and a frequency restoration method, and consider disturbances and actuator faults by using the sliding mode control for islanded microgrids. In [21], a solution by which to enhance the restoration capability of the distribution power system based on microgrids using a spanning tree search strategy is studied.

It is difficult to employ heuristic methods for the development of EMSs for microgrids that are able to participate in the day-ahead market [22] while considering the uncertainties of possible power grid-outages. MPC (Model Predictive Control) controllers have been widely used as a framework in which to solve complex problems in industry, and have recently drawn the attention of researchers studying microgrids [4,23]. This technique, which is a family of control methods, makes it possible to optimize a multi-objective cost function in which the future behavior of the microgrid components, energy forecast and price prediction can be easily integrated into the controller as constraints. Its stochastic formulation allows the management of uncertainties and the integration of different possible optimization scenarios [24], while its hybrid formulation makes it possible to deal with logic and continuous variables [4]. A complete framework with which to introduce microgrids into the electrical markets using hybrid MPC is carried out in [17,19]. Examples of the use of SMPC when applied to microgrids can be found in [25–27], while a far-reaching discussion on the advantages of the use of MPC for microgrids can be found in [4,17,19].

1.2. Main contributions

The state of the art of algorithms applied to the day-ahead schedule of microgrids is focused principally on a single optimization scenario under normal operation conditions in the grid-connected mode. The inclusion of aspects concerning a possible islanded-mode transition at each sample instant has barely been studied to date, despite being one of the most important functionalities of microgrids. The possibility of a transition toward an islanded mode owing to the occurrence of

Table 1
Operation aspects related to lifetime of Li-Ion batteries and hydrogen ESS [19].

ESS	Degradation issues
Batteries	Working cycles, overcharge, undercharge, high stress current ratio
Electrolyzer and fuel cells	Working hours, Fluctuations of current, start/stop cycles

power grid outages becomes relevant when the microgrid has to feed critical loads. This kind of loads is frequently found in facilities such as hospitals, technological centers or universities, transport stations, military installations, etc., which are usually characterized by a having reduced amount of space in which to locate energy storage systems, while high autonomy is simultaneously required by the ESS operated in islanded mode. There is, however, a lack of literature concerning the introduction of resiliency criterion into the schedule of microgrids.

The hybridization of ESS is an issue that has not previously been studied in those papers whose research is based on the enhancement of microgrid resiliency. As stated in [28], the hybridization of energy storage technologies can provide additional flexibility and competitiveness to microgrids. Several energy storage options are currently available, and it is important to highlight the great potential of hydrogen as an energy carrier. As occurs with batteries, hydrogen ESS have both advantages and drawbacks.

As can be seen in Fig. 1, batteries and hydrogen ESS are complementary technologies. While batteries have a better power density ratio, hydrogen achieves a better energy density. As discussed in [4], power density aspects are related to a faster transient response, whereas higher energy density achieves longer autonomy. The combination of both technologies enhances the autonomy of the microgrid in off-grid periods, thus achieving an appropriate transient response and decreasing the physical space required to store energy. As detailed in Table 1, the operation costs and degradation issues of batteries and hydrogen ESS are complementary. The development of advanced EMSs for microgrids that include the operation and degradation cost of each storage technology would, therefore, increase the economic competitiveness of the whole ESS.

When compared to a battery ESS, a hydrogen ESS allows a decoupling between the installed power of the storage system and the energy storage capacity. The stored energy depends on the size of the storage tank, and it is also possible to compress the hydrogen at a high pressure, and even liquefy it in order to have a larger quantity of stored energy while using a similar space. This allows large amounts of energy to be stored using materials that cost less than those that would be required in order to achieve a similar energy storage capacity when using batteries. In addition to this, it should be pointed out that batteries require much more space than hydrogen tanks. As shown in Fig. 1, the use of hybrid ESS [29,30] based on both batteries and hydrogen tanks stands out as a feasible solution to the space problem in the aforementioned facilities, which ultimately leads to a significant increase in the energy density of the whole ESS. Since batteries can compensate the lower power density of hydrogen, a hybrid scheme results in both a higher energy density and a higher power density ESS. These technologies are also complementary as regards the degradation issues [31,32], which affect the lifetime of the whole ESS, as summarized in Table 1.

The works carried out in [18,19] are focused on the development of a two-level MPC-based EMS strategy oriented toward the optimization of a microgrid with a hybrid ESS, thus minimizing the degradation cost and the operational cost of the whole ESS. The schedule carried out in the first control level is detailed in [18], while [19] describes a second stage in which a real-time controller is developed by following the schedule carried out in the first stage.

The Interreg SUDOE European Project IMPROVEMENT (Integration of combined cooling, heating and power (CCHP) microgrids in zero-energy public buildings under high power quality and continuity

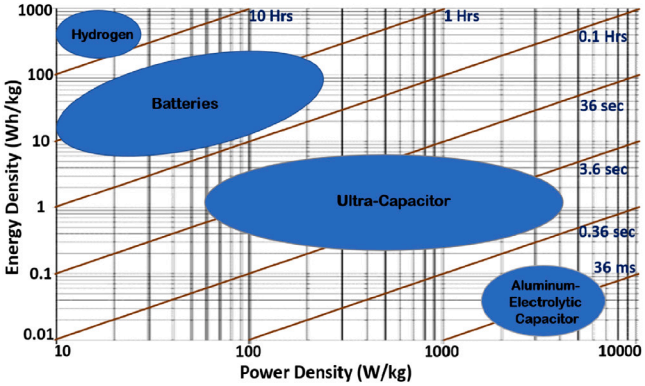

Fig. 1. Power and energy density for batteries and hydrogen.

requirements) is focused on reconverting existing public buildings with critical loads into Zero Energy Buildings by means of the integration of CCHP microgrids using hybrid ESS. The principal objective of the work presented herein, which is being conducted under the framework of the IMPROVEMENT project, is the development of a power-grid-fault-resilient EMS with which to optimize the participation of microgrids in the day-ahead electrical market so as to guarantee the supply of critical loads of electricity, considering possible power grid blackouts at all the sample instants of the schedule horizon. In order to accomplish this objective, this paper enhances the works carried out in [17,18] by including the uncertainty of possible grid blackouts at any of the sample periods considered in the day-ahead optimization of the microgrid. In [18], the uncertainties in the energy prediction were introduced in the EMS integrating an uncertainty band to the energy forecast. The optimization is carried out considering a pessimistic scenario and an optimistic one which are solved at the same time, by imposing to the controller that in both scenarios the energy exchange with the main grid has to be similar. In this work, the procedure explained in [17,18] is improved considering a possible transition from the grid-connected mode to the islanded mode at all the optimization instants of the day-ahead schedule, taking into account only the pessimistic scenario used in [18]. Once the optimization is performed, the obtained schedule is applied to the real-time control procedure exposed in [19]. The results obtained demonstrate that the microgrid operation in the day-ahead market guarantees the electrical supply of critical loads, even under power grid blackout conditions, at all the sample instants of the considered schedule horizon. Some of the features of the proposed algorithm, which are considered as the main highlights of the present work, are the following ones:

- The algorithm optimizes the minimum level of energy stored by each ESS technology (batteries and hydrogen), considering a possible transition to the islanded mode at each sample instant of the schedule horizon (SH) of the day-ahead market considered. These minimum levels of energy stored in each technology were optimally calculated by taking the associated operation cost of each technology into account, in addition to including possible degradation issues.
- In order to increase the versatility of the application, two resilience criteria were included: (i) supplying energy to the maximum number of loads in the case of grid blackouts during an established period (Survivability criterion), and (ii) ensuring that critical loads can be fed during a complete day (Criticality criterion), even in the case of instants that may occur after the final instant of the day-ahead schedule, considering the normal operation of the microgrid (grid-connected mode).
- The proposed methodology includes a formulation with which to carry out load and generation curtailment processes when the microgrid works in islanded mode.

Table 2
Summary of main microgrid schedule methods compared with the main features integrated into the controller proposed in this paper.

Hour	[2], [5]–[10]	[4], [17], [19]	[14]–[16]	[25], [26], [27]
Microgrid resilience	✓		✓	
Grid energy exchange		✓		✓
Survivability of loads			✓	
Hybrid ESS		✓		✓
ESS degradation cost		✓		
EMS fault tolerance control	✓			
Stochastic MPC		✓		✓

The main innovation as regards the approaches presented in this work is based on the optimization of the use of hybrid ESS by calculating, at each sample instant, the optimal minimum level of the State of Charge (SOC) for the batteries and the Level of Hydrogen (LOH) of the tank in order to guarantee the electrical supply of critical loads in the case of grid outages. Table 2 provides a summary of the different characteristics integrated into the controller developed in this paper and compares them to those in the existing literature, highlighting the contributions provided by this paper.

1.3. Structure and organization of the paper

The remainder of the paper is organized as follows: Section 2 shows the formulation of the SMPC-based controller, while the principal results obtained for the controller are presented and discussed in Section 3. Finally, Section 4 outlines the main conclusions of the paper.

2. Stochastic MPC-based controller design

The microgrid studied herein is shown in Fig. 3. As can be seen, it is composed of wind turbine and photovoltaic generators, it contains critical and non-critical loads and there are two kinds of ESS: batteries and hydrogen. The difference between critical and non-critical loads is given by the consequences of not being able to feed them. Therefore, non-critical loads will be those ones, that in the case of not being fed, will represent an economic damage which is assumable. On the contrary, the critical loads will be those that, if they do not receive power supply will not only supposes economic losses as the previous ones, but could also affect the health of people, the security and defense of facilities or the development of research. The power exchange with the main grid is carried out using an Intelligent Power Switch (IPS), which is normally closed. Under grid outage conditions or in those cases in which the power quality required cannot be satisfied in grid-connected mode, the IPS is opened and the microgrid works in islanded-mode. The block diagram (BD) of the controller is shown in Fig. 2. As can be seen, the BD is composed by four sub-blocks: (i) Forecast Module, (ii) Plant Model, (iii) Resilience MPC-Controller and (iv) Economic MPC-Controller. Throughout this section, the corresponding details for each block can be found separately in the different subsections.

2.1. General terms and design criteria

The controller is designed to allow the microgrid to participate in the Day-Ahead Market, and the sample time considered is, therefore, Ts=1 h.

The controller is designed according to the following concepts previously introduced in the existing literature related to microgrid resilience:

1. *Feasible Islanding/Criticality Criterion*: This is defined as the ability of the microgrid controller to take into account that, in the case of a grid outage, it will be able to supply energy to at least its most critical loads [2] during a similar period of the SH considered, after the blackout event occurs.

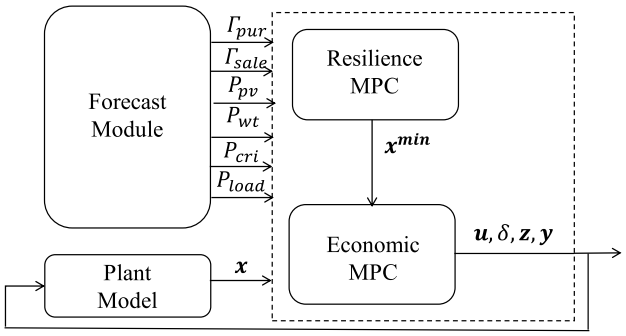

Fig. 2. Block diagram of the MPC.

2. *Survivability Criterion*: Capacity to feed the maximum number of loads, with it being necessary to ensure critical loads during an established survivability period [2]. Notice that to feed all the loads of the microgrid during the complete schedule horizon of the day-ahead optimization of the microgrid considering possible power grid blackouts could be possible; however, it would require a large investment in the capacity of the energy storage systems. For this reason, in this case study, the survivability criterion is only maintained for two hours after the transition to the islanded mode of the microgrid, in coincidence with the average time that electricity distribution companies usually take to re-establish the electrical service (Spain is taken as reference country for the developments carried out in this paper). Nevertheless, the survivability horizon can be expanded to periods longer than two hours following a similar procedure.
3. *Economic Competitiveness of the ESS*: Integration of the safe operation of the ESS in order to avoid degradation or failure conditions. Minimization of the degradation issues and operation costs associated with the hybrid ESS.

In order to introduce the fact that a grid blackout could occur at each sample instant, a different optimization scenario is considered for each sample instant of the SH, considering a transition between the grid-connected to the islanded mode at the aforementioned sample instant. These scenarios are defined as 'critical scenarios' and are solved in the 'Resilience MPC' module of the BD. Finally, one 'normal' scenario is included in order to optimize the participation of the microgrid in the day-ahead market when it is working in the grid-connected mode for all the sample instants of the SH. This is optimized in the 'Economic MPC' module of the controller. The control problem can be formulated as a Stochastic Multi-Scenario MPC controller by employing the sum of a multi-objective cost function for each scenario, as shown in (1), in which the upper-index $[s]$ is used to refer to each scenario considered, where N_s is the number of optimization scenarios. Each cost function $J^{[s]}$ can be expressed as a function of a set of continuous control variables $\mathbf{u}$, a set of logical variables $\boldsymbol{\delta}$ and a set of mixed variables $\mathbf{z}$ (defined as the product of one logic and one continuous variable [33]). These variables are subjected to a set of constraints concerning their physical bounds (2)–(4), which also have to be integrated into the controller. These control variables produce a set of system outputs $\mathbf{y}$ which are also subjected to physical limits (6). The different control variables and system outputs are related to a physical model of the plant, which is modeled using the space state representation of the plant by introducing a set of state variables $\mathbf{x}$ (defined as those variables whose value depends on that obtained at the previous sample instant). Owing to the presence of continuous, logic and mixed variables, the state space model representation will be modeled using the MLD framework as shown in expressions (7)–(9), where $\mathbf{d}$, unlike $\mathbf{u}$, represents disturbances or non-manipulate variables. A, B, C, D and E are the

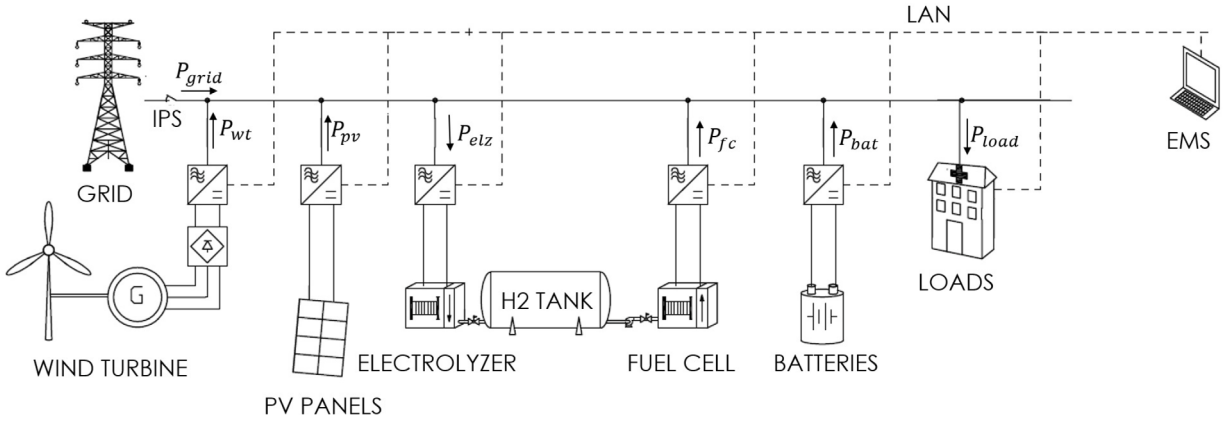

Fig. 3. Microgrid considered in this paper.

matrices used to define the relationships among the different variables which integrate the state space representation of the microgrid.

$$\min J = \sum_{s=1}^{N_s} J^{[s]}(\mathbf{u}^{[s]}, \boldsymbol{\delta}^{[s]})$$
$$J^{[s]} = \sum_{k=1}^{SH} f(\mathbf{u}^{[s]}(t+k), \boldsymbol{\delta}^{[s]}(t+k)) \quad (1)$$

subject to:

$$\mathbf{u}^{min} \leq \mathbf{u}^{[s]}(t) \leq \mathbf{u}^{max} \quad (2)$$
$$0 \leq \boldsymbol{\delta}^{[s]}(t) \leq 1 \quad (3)$$
$$0 \leq \mathbf{z}^{[s]}(t) \leq \mathbf{z}^{max} \quad (4)$$
$$\mathbf{x}^{min} \leq \mathbf{x}^{[s]}(t) \leq \mathbf{x}^{max} \quad (5)$$
$$\mathbf{y}^{min} \leq \mathbf{y}^{[s]}(t) \leq \mathbf{y}^{max} \quad (6)$$

$$\mathbf{x}^{[s]}(t+1) = \mathbf{A}\mathbf{x}^{[s]}(t) + \mathbf{B}_u\mathbf{u}^{[s]}(t) + \mathbf{B}_\delta\boldsymbol{\delta}^{[s]}(t) + \mathbf{B}_z\mathbf{z}^{[s]}(t) + \mathbf{B}_d\mathbf{d}(t) \quad (7)$$
$$\mathbf{y}^{[s]}(t) = \mathbf{C}\mathbf{x}^{[s]}(t) + \mathbf{D}_u\mathbf{u}^{[s]}(t) + \mathbf{D}_\delta\boldsymbol{\delta}^{[s]}(t) + \mathbf{D}_z\mathbf{z}^{[s]}(t) + \mathbf{D}_d\mathbf{d}(t) \quad (8)$$
$$\mathbf{E}_\delta\boldsymbol{\delta}^{[s]}(t) + \mathbf{E}_z\mathbf{z}^{[s]}(t) \leq \mathbf{F}\mathbf{x}^{[s]}(t) + \mathbf{E}_u\mathbf{u}^{[s]}(t) + \mathbf{E}_d\mathbf{d}(t) \quad (9)$$

The microgrid studied herein can be modeled with its state-space representation by using the following arrays for each scenario:

$$\boldsymbol{u}^{[s]} = \left[P_{ch}^{[s]}, P_{dis}^{[s]}, P_{elz}^{[s]}, P_{fc}^{[s]}, P_{pur}^{[s]}, P_{sale}^{[s]}, \alpha_{cur\_gen}^{[s]}\right]^T \quad (10)$$

where $P_{ch}^{[s]}$, $P_{dis}^{[s]}$ are variables with only positive values for the charging and discharging power setpoints sent to the batteries, $P_{elz}^{[s]}$ and $P_{fc}^{[s]}$ are the reference power values provided by the micro-grid controller to the internal controllers of the electrolyzer and fuel cell, respectively. $P_{pur}^{[s]}$, $P_{sale}^{[s]}$ are also variables with only positive values that are used to calculate the optimal power exchange with the main grid during the selling and purchasing processes. The wind turbine and the photovoltaic generator have a control with which to regulate the power they generate. This power variation is controlled by a coefficient signal defined by $\alpha_{cur\_gen}^{[s]} \in [0, 1]$.

$$\boldsymbol{\delta}^{[s]} = [\delta_{ch}^{[s]}, \delta_{dis}^{[s]}, \delta_{elz}^{[s]}, \delta_{fc}^{[s]}, \sigma_{elz}^{[s]}, \sigma_{fc}^{[s]}, \chi_{elz}^{[s]}, \chi_{fc}^{[s]}, \delta_{cur,1}^{[s]}, \delta_{cur,2}^{[s]}, \dots \delta_{cur,10}^{[s]},]^T \quad (11)$$

$\delta_{ch}^{[s]}$ is active for the charging process of the battery while $\delta_{dis}^{[s]}$ is "1" when the batteries are discharging. The electrolyzer and fuel cell have logic signals associated with their on/off-state, which are defined with $\delta_{elz}^{[s]}$ and $\delta_{fc}^{[s]}$. $\sigma_{elz}^{[s]}$ and $\sigma_{fc}^{[s]}$ are auxiliary variables that are linked with the start-up processes of the electrolyzer and the fuel cell, while $\chi_{elz}^{[s]}$ and $\chi_{fc}^{[s]}$ are auxiliary variables that define those instants at which the electrolyzer and the fuel cells are in on-state but are being switched on/off. Finally, $\delta_{cur,1}^{[s]}, \delta_{cur,2}^{[s]}, \dots \delta_{cur,10}^{[s]}$ are logic variables associated with the load curtailment applied to different groups of loads.

$$\mathbf{z}^{[s]} = \left[z_{ch}^{[s]}, z_{dis}^{[s]}, z_{elz}^{[s]}, z_{fc}^{[s]}, \vartheta_{elz}^{[s]}, \vartheta_{fc}^{[s]}\right]^T \quad (12)$$

where $z_{dis}^{[s]}$, $z_{ch}^{[s]}$, $z_{elz}^{[s]}$ and $z_{fc}^{[s]}$ are the mixed product of the continuous and logic control variables of the charging and discharging of the batteries, the electrolyzer and the fuel cell , and $\vartheta_{elz}^{[s]}$ and $\vartheta_{fc}^{[s]}$ are the power increments in the electrolyzer and the fuel cell at all those instants at which they are active but in the switch on/off states.

The state variables of the microgrid are defined by the level of energy stored in the battery $SOC^{[s]}$ and in the hydrogen tank $LOH^{[s]}$ (13).

$$\mathbf{x}^{[s]} = \left[SOC^{[s]}, LOH^{[s]}\right]^T \quad (13)$$

The outputs of the plant are defined with the power exchanged with the main grid $P_{grid}^{[s]}$ (14).

$$\mathbf{y}^{[s]} = \left[P_{grid}^{[s]}\right]^T \quad (14)$$

In the case of being either islanded or isolated from the main grid, the formulation would be similar, but the constraint $P_{grid}^{[s]} = 0$ would be introduced.

2.2. Forecast module

In this module, the prediction the disturbance array $\mathbf{d}$ is obtained by the prediction carried out in the Forecast Module of the controller using the methodology defined in [17]. The following disturbance array is incorporated into the controller:

$$\mathbf{d} = \left[\hat{P}_{pv}, \hat{P}_{wt}, \hat{P}_{load}, \hat{P}_{cri}\right]^T \quad (15)$$

where the energy generation forecasted for the photovoltaic and wind turbine generators is defined by $(\hat{P}_{pv}(t), \hat{P}_{wt}(t))$, and the consumption in the microgrid is provided by the global load $\hat{P}_{load}(t)$, which is composed of different load groups that can be disconnected from the microgrid if necessary. The load curtailment process is carried out by defining different priority levels. Maximum priority is given to the so-called 'critical loads' $P_{cri}(t)$, which have to be continuously fed. This module also predicts the cost of the processes of purchasing energy from and selling it to the main grid $(\hat{\Gamma}_{pur}(t), \hat{\Gamma}_{sale}(t))$.

2.3. Plant model

The constraints shown in (7) regarding the state variables of the plant can be particularized for this controller by employing (16) and

(17), where C_{bat} is the capacity of the battery and the coefficients η_α represent the efficiencies.

$$SOC^{[s]}(t+1) = SOC^{[s]}(t) + \frac{z^{[s]}_{ch}(t)\cdot\eta_{ch}}{C_{bat}} - \frac{z^{[s]}_{dis}(t)/\eta_{dis}}{C_{bat}} \tag{16}$$

$$LOH^{[s]}(t+1) = LOH^{[s]}(t) + z^{[s]}_{elz}(t)\cdot\eta_{elz} - \frac{z^{[s]}_{fc}(t)}{\eta_{fc}} \tag{17}$$

The constraints expressed in (8) are obtained by employing the energy balance constraints (18) and (19).

$$\begin{aligned} &P^{[s]}_{pur}(t) - P^{[s]}_{sale}(t) + \hat{P}_{pv}(t) + \hat{P}_{wt}(t) + z^{[s]}_{dis}(t) - z^{[s]}_{ch}(t) \\ &+ z^{[s]}_{fc}(t) - \hat{P}_{load}(t) - z_{elz}(t) + \sum_{n=1}^{10}(\delta^{[s]}_{cur,n}(t)\hat{P}_{load,n}(t)) \\ &- \alpha^{[s]}_{cur,gen}(t)\cdot(\hat{P}_{pv}(t) + \hat{P}_{wt}(t)) = 0 \end{aligned} \tag{18}$$

$$-P^{[s]}_{grid}(t) + P^{[s]}_{pur}(t) - P^{[s]}_{sale}(t) = 0 \tag{19}$$

2.4. Resilience MPC-controller block

The main aim of this block is to optimize the minimum level of energy stored in order to achieve the criteria regarding survivability and criticality. Fig. 4 represents the tree of possible scenarios when considering a possible grid blackout for each sample instant of the SH. As can be seen in the figure, depending on the scenario considered, each sample instant can be categorized as: (1) 'Normal': it is possible to exchange energy with the main grid, (2) 'Survivability': at this sample instant, the criterion of survivability and criticality have to be integrated into the control problem, and (3) 'Criticality': there is no connection with the main grid, but only the critical loads have to be fed. As can be seen in the tree diagram of the scenarios represented in Fig. 4, the SH of the optimization varies. When the schedule horizon of the normal scenario is SH, if the grid blackout occurs at the sample instant k, the schedule horizon of the control problem associated with this scenario is $SH+k$ in order to guarantee the criticality for a period similar to the SH considered for the normal scenario. The survivability criterion are considered only for two successive sample instants after the grid outage. Note that each of the scenarios considered that is solved by the Resilience MPC block can be optimized as an independent problem.

$$\begin{aligned} J^{[s=j]} = T_s \underbrace{\left(w_{SOC}\cdot SOC^{[j]}(t_j) + w_{LOH}\cdot LOH^{[j]}(t_j)\right)}_{Minimum\ Storage\ Level\ Calculus} + \\ \sum_{k=1}^{k=SH+j} \underbrace{\left(-\Gamma^{DM}_{sale}(t_k)\cdot z^{[j]}_{sale}(t_k) + \Gamma^{DM}_{pur}(t_k)\cdot z^{[j]}_{pur}(t_k)\right)}_{Grid\ Exchange\ Revenue\&Cost(J_{grid})} \\ + \underbrace{10\cdot\max(\Gamma^{DM}_{sale}(t_k \le t_j))\cdot\alpha^{[j]}_{cur,gen}(t_k)}_{Generation\ Curtailment\ Cost} \\ + \underbrace{\sum_{i=1}^{i=10}\left((10+i)\cdot\max(\Gamma^{DM}_{pur}(t_k \le t_j))\cdot\delta^{[j]}_{cur,load\_i}(t_k)\right)}_{Load\ Curtailment\ Cost} \\ + \underbrace{\frac{CC_{bat}}{2\cdot Cycles_{bat}}\sum_{\alpha=ch,dis}\left(z^{[j]}_{bat,\alpha}(t_k)\right)}_{Batteries\ Cycling\ Cost} \\ + \underbrace{\sum_{\alpha=ch,dis}(Cost_{degr,\alpha}\cdot(z^{[j]}_{bat,\alpha}(t_k))^2)}_{Batteries\ ESS\ Degradation} \\ + \underbrace{\sum_{\alpha=elz,fc}\left(\left(\frac{CC_\alpha}{Hours_\alpha} + Cost_{o\&m,\alpha}\right)\delta^{[j]}_\alpha(t_k)\right.}_{Hydrogen\ ESS\ Hourly\ Cost\ Use} \\ \underbrace{\left.+Cost_{startup,\alpha}\cdot\sigma^{[j]}_\alpha(t_k) + Cost_{degr,\alpha}\cdot(\vartheta^{[j]}_\alpha(t_k))^2\right)\Big)}_{Hydrogen\ ESS\ Degradation} \end{aligned} \tag{20}$$

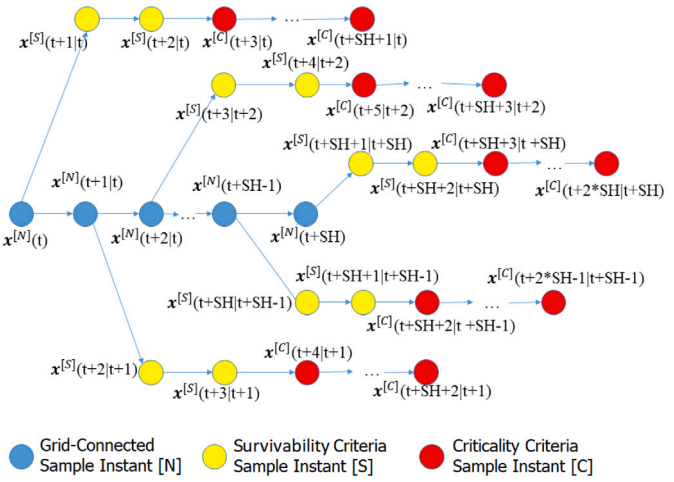

Fig. 4. Scenarios Tree Diagram considering a possible power grid outage at each sample instant of the day-ahead market participation.

Subject to:

$$\begin{aligned} &P^{[j]}_{grid}(t_k) = 0 \quad \forall k > j \\ &\alpha^{[j]}_{cur,gen\_i}(t_k) = 0 \quad \forall k \le j \\ &\delta^{[j]}_{cur,load\_i}(t_k) = 0 \quad \forall k \le j \\ &\delta^{[j]}_{cur,load\_i}(t_k) = 1 \quad \forall k > j+2 \end{aligned} \tag{21}$$

The cost function for the scenario which considers that the grid outage occurs at the sample instant j is shown in (20) (please note that there is a different scenario 'j' for all the sample instants of the SH) and is subjected to the specific constraints expressed in (21). The nomenclature t_k is utilized, which represents $t+k$. In this cost function, there are different expressions that refer to optimization objectives. The first and most important term of the cost function is related to the ESS storage level, where w_{SOC} and w_{LOH} are weighting factors with higher values in the cost function. The objective of this term is to minimize these LOH and SOC values, thus satisfying the survivability and criticality criteria for all the sample instants after that at which the grid power connection is lost. The second term in the cost function concerns the grid exchange revenue and will depend on the sale and purchase prices in the Day-Ahead Market (DM) Γ^{DM}_{pur} and Γ^{DM}_{sale}. Note that this expression will be 0 if the outage is produced (when k>j, as stated in (21)).

The third term of the cost function manages the generation curtailment. In order to penalize this process rather than exchanging energy at instants prior to the grid blackout, the weighting cost is 10 times greater than the maximum DM sale price forecast at the sample instants prior to the outage. The same procedure is carried out for the load curtailment. The action of disconnecting a group of loads is penalized in the sample instants of survivability or normal criteria. In this case, the load groups (only the non-critical loads, because the critical loads cannot be shut down) have been divided into different levels (δ_i, in this case i = 10), and different priority levels have been assigned to them.

The cost of using the batteries is divided into two different expressions. It is known that the useful life of the batteries depends on the number of charging/discharging cycles. This aspect is integrated into the cost function by means of the parameters CC_{bat}, the capital cost of acquiring the battery, and the number of life cycles ($Cycles_{bat}$) guaranteed by the manufacturer of the batteries. Furthermore, during the continuous operation of the battery, its lifetime can be reduced if high stress charging/discharging current is applied, and the charging and discharging power of the batteries is, therefore, quadratically penalized [17]. The hydrogen ESS is similarly divided into two costs. Unlike the battery, ESS hydrogen life cannot be measured by operating

cycles, but is rather measured by operating hours and its operation and maintenance $\text{Cost}_{o\&m}$, where $\delta_\alpha = 1$ at those sample instants at which the fuel cell or the electrolyzer are working. The degradation cost in this case depends on two factors [17]: the degradation processes associated with the start-up/shut-down, where σ_α is the start-up state of the electrolyzer and the fuel cell. There is also a degradation cost depending on the power fluctuations ϑ_α applied to these devices at all the instants at which they are active, with the exception of the sample instants at which they are switched on or switched off. The controller has to take into account the constraints related to the state space of the microgrid expressed in (7)–(9).

Electrolyzer and fuel cell manufacturers recommend keeping these devices working in a power range of 10%–100% of their maximum power, which is why the fuel cells and the electrolyzer are formulated using logical and continuous variables (δ_α, P_α), being $z_\alpha = P_\alpha \cdot \delta_\alpha$. Please note that $\delta(t)$ can take a value of 0, resulting in the possibility of having 3 different operating limits $[0, P_\alpha^{min}, P_\alpha^{max}]$.

With regard to the degradation of the electrolyzer and the fuel cell owing to start-up and shut-down cycles, this is quantified in the controller using the auxiliary logic variables $\sigma_\alpha(t)$.

Another issue that can cause the electrolyzer and the fuel cell to undergo degradation is power fluctuation at those instants at which these devices are active, except when they are switched on or off. These processes are integrated into the controller by employing the mixed variable ϑ_α.

The different weighting factors have been selected according to certain economic factors outlined in the methodology indicated in Ref. [17], such as the capital cost of the devices, lifetime, etc. Their values are shown in Table 3. The parameters w_{SOC} and w_{LOH} are adjusted once the remaining weights have been set, since both parameters are the most restrictive criteria in the cost function. The system must feed all the loads before the outage, and the weighting factors for load and generation curtailment have, therefore, been included in order to avoid using them when the selling and purchasing processes are available. In the case of generation curtailment, the weighting factor utilized has been assigned with one order of magnitude higher than the maximum selling price before the outage event occurs. The system will, therefore, prioritize the sale of excess of energy before carrying out a curtailment generation. The generation curtailment will consequently occur only after the outage takes place and the ESS reaches its maximum capacity. A similar procedure was followed with the weighting factors utilized for the load curtailment in order to prioritize the energy purchase at any time before the outage is considered over a curtailment in load because the minimum level of energy capacity in the ESS has been reached. Due to the presence of continuous and logic variables, the expressions provided in (9) can be obtained by transforming the logic relationships between the variables $\mathbf{u}$, $\boldsymbol{\delta}$ and $\mathbf{z}$, following the procedure defined in [33]. The start-up states $\sigma_{elz}^{[s]}$ and $\sigma_{fc}^{[s]}$ can be related to $\delta_{elz}^{[s]}$ and $\delta_{fc}^{[s]}$ by utilizing the logic relationships expressed in (22), which can be linearized as constraints using the expressions (23)–(25).

$$\sigma_\alpha^{[s]}(t) = \delta_\alpha^{[s]}(t) \wedge \sim \delta_\alpha^{[s]}(t-1)|_{\alpha=elz,fc} \tag{22}$$

$$m \leq -\delta_\alpha^{[s]}(t) + \sigma_\alpha^{[s]}(t) \leq 0|_{\alpha=elz,fc} \tag{23}$$

$$m \leq -(1-\delta_\alpha^{[s]}(t-1)) + \sigma_\alpha^{[s]}(t) \leq 0|_{\alpha=elz,fc} \tag{24}$$

$$m \leq \delta_\alpha^{[s]}(t) + (1-\delta_\alpha^{[s]}(t-1)) - \sigma_\alpha^{[s]}(t) \leq 1|_{\alpha=elz,fc} \tag{25}$$

where the symbols $\wedge$ and $\sim$ represent the logic operations AND and NOT, respectively. The relation between $\chi_{elz}(t)$ and $\delta_{elz}(t)$ is defined in (26), which can be introduced into the controller using the constraints (27)–(29):

$$\chi_\alpha^{[s]}(t) = \delta_\alpha^{[s]}(t) \wedge \delta^{[s]} a_\alpha(t-1)|_{\alpha=elz,fc} \tag{26}$$

$$m \leq -\delta_\alpha^{[s]}(t) + \chi_\alpha^{[s]}(t) \leq 0|_{\alpha=elz,fc} \tag{27}$$

$$m \leq -\delta_\alpha^{[s]}(t-1) + \chi_\alpha^{[s]}(t) \leq 0|_{\alpha=elz,fc} \tag{28}$$

$$m \leq \delta_\alpha^{[s]}(t) + \delta_\alpha^{[s]}(t-1) - \chi_\alpha^{[s]}(t) \leq 1|_{\alpha=elz,fc} \tag{29}$$

$$z_\alpha^{[s]}(t) = P_\beta^{[s]}(t) \cdot \delta_\alpha^{[s]}(t) \tag{30}$$

$$m \leq z_\alpha(t) - P_\alpha^{max}\delta_\alpha^{[s]}(t) \leq 0 \tag{31}$$

$$0 \leq z_\alpha^{[s]}(t) - P_\alpha^{min}\delta_\alpha^{[s]}(t) \leq M \tag{32}$$

$$P_\beta^{[s]}(t) - P_\alpha^{max}(1-\delta_\alpha^{[s]}(t)) - z_\alpha^{[s]}(t) \leq 0 \tag{33}$$

$$0 \leq P_\alpha^{[s]}(t) - P_\alpha^{min}(1-\delta_\alpha^{[s]}(t)) - z_\alpha^{[s]}(t) \tag{34}$$

The corresponding mixed products related to the charging and discharging of the batteries, the electrolyzer and the fuel cell can be defined by employing the mixed product mentioned in (30), which can be transformed into the linear constraints defined in (31)–(34) by replacing $\alpha = \{elz, fc, ch, dis\}$ and $\beta = \{elz, fc, bat, bat\}$ being $P_{ch}^{max} = -P_{bat}^{min}$, $P_{dis}^{max} = P_{bat}^{max}$ and $P_{ch}^{min} = P_{dis}^{min} = 0$. The constants m and M represent the minimum/maximum possible value on the control platform. Finally, the next constraints are included in order to avoid inefficient energy processes as the charging of the batteries by the use of the fuel cell or the hydrogen production of the electrolyzer through the battery discharge:

$$0 \leq \delta_\alpha + \delta_\beta \leq 1|_{\alpha=dis,ch}^{\beta=elz,fc} \tag{35}$$

Finally, $\vartheta_\alpha(t)$ is defined as a mixed product shown in (36), which is integrated into the controller using the linear constraints provided in (37)–(40), where $\alpha = \{elz, fc\}$.

$$\vartheta_\alpha(t) = (P_\alpha(t) - P_\alpha(t-1)) \cdot \chi_\alpha(t) \tag{36}$$

$$m \leq \vartheta_\alpha(t) - \Delta P_\alpha^{max}\chi_\alpha(t) \leq 0 \tag{37}$$

$$0 \leq \vartheta_\alpha(t) - \Delta P_\alpha^{min}\chi_\alpha(t) \leq M \tag{38}$$

$$m \leq \vartheta_\alpha(t) - \Delta P_\alpha(t) + \Delta P_\alpha^{min}(1-\chi_\alpha(t)) \leq 0 \tag{39}$$

$$0 \leq \vartheta_\alpha(t) - \Delta P_\alpha(t) + \Delta P_\alpha^{max}(1-\chi_\alpha(t)) \leq M \tag{40}$$

The complexity and computation time required in order to find the optimal solution for a Multi-scenario SMPC controller increases with the number of scenarios considered (N_s). In the case study, one normal scenario and one critical scenario is associated with each sample instant of the SH given for the normal scenario. In order to optimize the time required, the control problem is decomposed into each of the critical scenarios considered. Owing to the fact that only the state variables of the SMPC-controller depend on its value obtained at the previous sample instant, as a first step of the algorithm, the minimum value of $\mathbf{x}$ that is required is calculated for each critical scenario. The most restrictive value of $\mathbf{x}$ obtained for each sample instant from all the critical scenarios is later imposed as a system constraint for the normal scenario optimization problem. Note that the cost function of the Resilience MPC Controller has to prioritize the autonomy of the system in order to feed the critical loads and to achieve the survivability criterion, while the Economic MPC Controller maximizes the revenue of participating in the Day-Ahead Market. They are, therefore, formulated as two different control problems with different cost functions and constraints.

2.5. Economic MPC-controller block

Once the previous block has obtained the results, these values are used to calculate the minimum values for the state variables $\mathbf{x}$ (see the constraint detailed in (5)) by the Economic MPC block. Notice that due to the same presence of the logic and dynamic variables, the corresponding constraints exposed in the expressions (22)–(40) have to be also included in this block. For the sake of simplicity, the uncertainties of the energy forecast are not included but it could be done following the procedure given in [18]. One fundamental difference is that the controller does not use the physical limits for the ESS as usually occurs

in literature. Each scenario of the Resilience MPC calculates a value for each sample instant of the scenario considered.

$$LOH_{const} = \begin{bmatrix} LOH_1^{[1]} & LOH_1^{[2]} & \dots & LOH_1^{[SH]} \\ LOH_2^{[1]} & LOH_2^{[2]} & \dots & LOH_2^{[SH]} \\ \dots & \dots & & \dots \\ LOH_{SH}^{[1]} & LOH_{SH}^{[2]} & \dots & LOH_{SH}^{[SH]} \end{bmatrix} \tag{41}$$

$$SOC_{const} = \begin{bmatrix} SOC_1^{[1]} & SOC_1^{[2]} & \dots & SOC_1^{[SH]} \\ SOC_2^{[1]} & SOC_2^{[2]} & \dots & SOC_2^{[SH]} \\ \dots & \dots & & \dots \\ SOC_{SH}^{[1]} & SOC_{SH}^{[2]} & \dots & SOC_{SH}^{[SH]} \end{bmatrix} \tag{42}$$

The LOH and SOC matrix previously obtained (41)–(42) will be the key to obtain the desired prediction in this part of the algorithm. In this case, the Economic MPC has only SH hours of the schedule horizon, and the LOH and SOC constraint matrix, therefore, has a dimension of $SH \text{x} SH$.

$$\begin{aligned} J = T_s \sum_{k=1}^{k=SH} & \underbrace{\left(-\Gamma_{sale}^{DM}(t_k)\cdot z_{sale}(t_k) + \Gamma_{pur}^{DM}(t_k)\cdot z_{pur}(t_k)\right)}_{Grid\ \ Exchange\ \ Revenue\&Cost(J_{grid})} \\ & + \underbrace{\frac{\text{CC}_{bat}}{2\cdot \text{Cycles}_{bat}} \sum_{\alpha=ch,dis} \left(z_{bat,\alpha}(t_k)\right)}_{Batteries\ \ Cycling\ \ Cost} \\ & + \underbrace{\sum_{\alpha=ch,dis} \left(\text{Cost}_{degr,\alpha}\cdot (z_{bat,\alpha}(t_k))^2\right)}_{Batteries\ \ ESS\ \ Degradation} \\ & + \underbrace{\sum_{\alpha=elz,fc} \left(\left(\frac{\text{CC}_\alpha}{\text{Hours}_\alpha} + \text{Cost}_{o\&m,\alpha}\right)\delta_\alpha(t_k)\right)}_{Hydrogen\ \ ESS\ \ Hourly\ \ Cost\ \ Use} \\ & \underbrace{+\text{Cost}_{startup,\alpha}\cdot \sigma_\alpha(t_k) + \text{Cost}_{degr,\alpha}\cdot (\vartheta_\alpha(t_k))^2\Big)\Big)}_{Hydrogen\ \ ESS\ \ Degradation} \\ & + \underbrace{w_{SOC}\cdot (SOC(SH) - SOC^{[ref]})}_{Future\ \ Uncertainties} \\ & + \underbrace{w_{LOH}\cdot (LOH(SH) - LOH^{[ref]})}_{Future\ \ Uncertainties} \end{aligned} \tag{43}$$

The cost function in this control block (43) includes the possibility of purchasing or selling energy by exchanging energy with the main grid at all the sample instants, and its principal objective is to optimize the economic revenue of exchanging energy with the main grid, thus minimizing the operation cost of the hybrid ESS. As the possibility of exchanging energy with the main grid exists for all the sample instants, there is no need to apply load or generation curtailment processes. It is also unnecessary to calculate the minimum value of energy stored at none sample instant, the remaining terms of the cost function are similar to that expressed in (20), as can be seen in (43). Since there is only one scenario in this case, the upper-index related to the considered scenario is not used. The state space constraints developed in the Resilience MPC Block are similar to those used in this controller. In order to guarantee the criticality and survivability criteria, only the lower bounds of the SOC and LOH for each sample instant have to be modified. The most restrictive values of the SOC and LOH for each sample instant of all the values obtained for each of the scenarios are selected and imposed on the controller as follows:

$$SOC^E(t_k) \le SOC^N(t_k) \le SOC^{max} \tag{44}$$

$$LOH^E(t_k) \le LOH^N(t_k) \le LOH^{max} \tag{45}$$

where $SOC^E(t_k)$ is the maximum value of the k row from the SOC matrix obtained in the Resilience MPC block, as shown in (46). The same procedure is followed to obtain $LOH^E(t_k)$.

$$SOC^E(t_k) = \max\left(\begin{bmatrix} SOC_k^{[1]} & SOC_k^{[2]} & \dots & SOC_k^{[SH]} \end{bmatrix}\right) \tag{46}$$

Table 3
Components of the microgrid.

Grid parameters	
P_{grid_min}: −40 kW	P_{grid_max}: 40 kW
Renewable energy parameters	
PV Pannels: 30 kWp	Wind turbine: 10 kW
Hydrogen ESS parameters	
Electrolyzer: 50 kW, Tank: 35 N m^3	Fuel cell: 20 kW
LOH_{max}: 35 N m^3	LOH_{min}: 5 N m^3
$Cost_{deg,elz}$: 0.0577 €/W, Hour = 10000 h	$Cost_{startup,elz}$ = 0.123 €
ς: 0.23 N m^3/kWh, CC = 8.22 €/kWh	$Cost_{o\&m,elz}$ = 0.002 €/h
$Cost_{deg,fc}$: 0.0018 €/W, Hour = 10000 h	$Cost_{startup,fc}$ = 0.01 €
ς: 1.320 N m^3/kWh, CC = 30 €/kWh	$Cost_{o\&m,fc}$ = 0.001 €/h
w_{LOH} = 10	
Batteries ESS parameters	
Battery: ±15 kW; ±55 kWh	w_{SOC} = 0.1
$Cost_{deg,ch}$: 10^{-9} €/W^2 h	$Cost_{deg,dis}$: 10^{-9} €/W^2 h
η_{ch}: 0.90	η_{dis}: 0.95
SOC_{max} = 100%	SOC_{min} = 25%

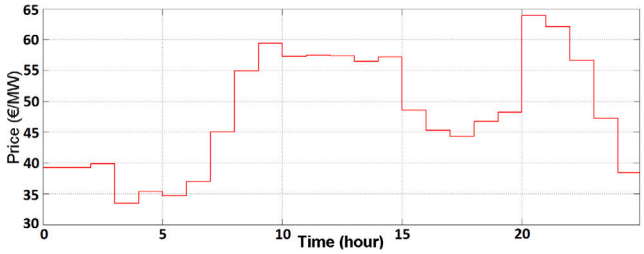

Fig. 5. Price prediction for day ahead.

3. Results

In this section, the controller is developed and validated by means of numerical simulations using the MATLAB® and TOMLAB® software as a solver tool. The total simulation execution took 530 s. The Resilience MPC Block performed 24 simulations, lasted 500 s, and each of the simulations lasted an average execution time of 21 s. The Economic MPC block executed the simulation in 30 s. The hardware used has the following characteristics: Intel® Core™ i7-6700 CPU @ 3.40 GHz, 16.0 GB RAM. The different components of the microgrid are specified in Table 3. The parameters and values integrated into the controller are shown in Table 3 and are based on [17].

The simulations were performed with a sample time of $T_s = 1$ hour and during a complete day, signifying $SH = 24$ hours. The data corresponding to the energy prices predicted and used in the forecast algorithm were based on the Iberian Market Operator history data on 05/04/20, as shown in Fig. 5.

The output obtained for each hour in the Resilience MPC block is composed of two figures. The first figure contains the power values obtained in the optimization for generation, loads, ESS and grid exchange for 24 h. The second represents the evolution of the LOH and SOC.

The results of the microgrid optimization under a grid fault condition for 4 different sample instants are shown in Figs. 6–10. It is important to state that in each figure, the grid is available only until the hour of the called "$Node$". $Node$ refers to a specific scenario in which a blackout in the main power grid occurs at this sample instant and the microgrid works as an islanded system. Moreover, in each scenario, the critical loads are fed during a period $SH + Node$, but the non-critical loads are present only until $Node + 2$, because the survivability criteria

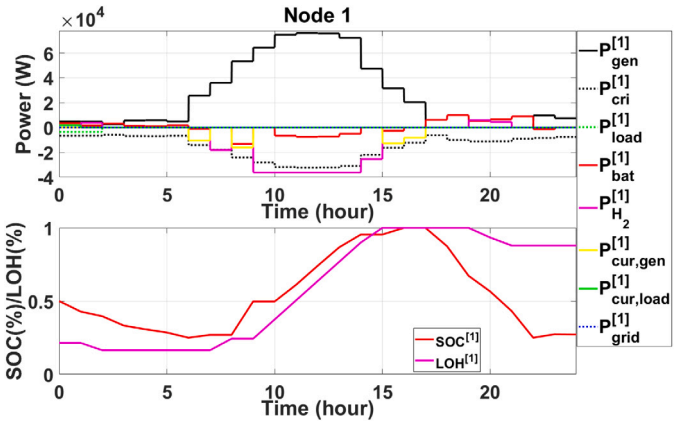

Fig. 6. Resilience MPC simulation in hour 1.

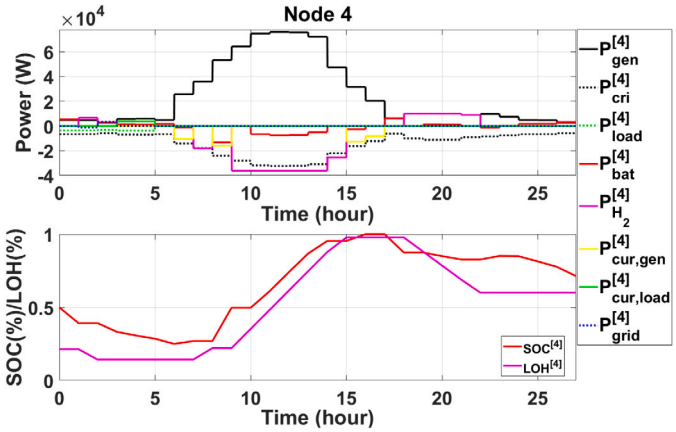

Fig. 7. Resilience MPC simulation in hour 4.

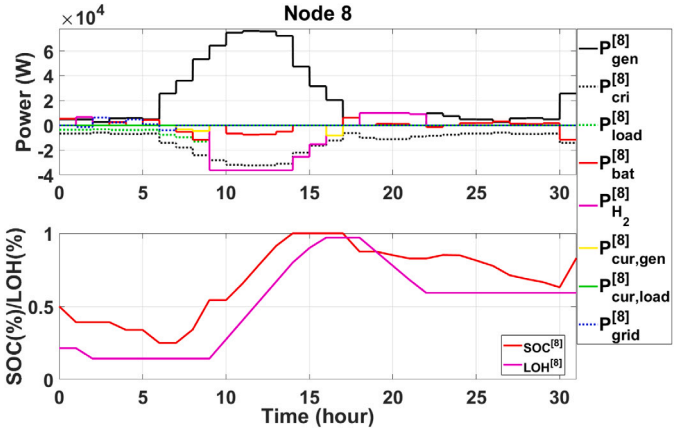

Fig. 8. Resilience MPC simulation in hour 8.

is established for 2 h after the fault occurs. The values of the SOC and LOH are integrated into the Matrix for each of these $Nodes$, as explained previously. The energy generated by the photovoltaic panels and the wind turbine are integrated into a common term $P_{gen} = P_{wt}+P_{pv}$ in the graphs.

Fig. 6 represents the case study for a grid outage at the sample instant $t = 1$ h. As can be seen the Node 1 shows that the microgrid has

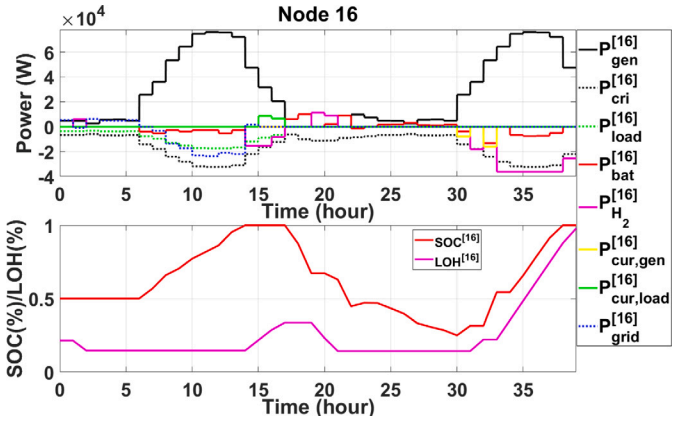

Fig. 9. Resilience MPC simulation in hour 16.

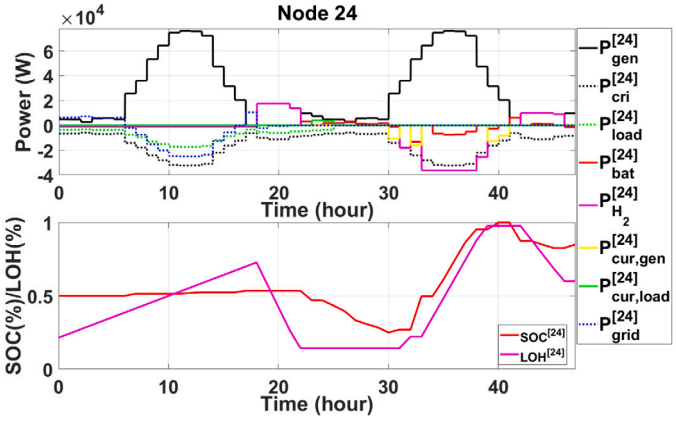

Fig. 10. Resilience MPC simulation in hour 24.

to cut some of the non-critical loads because the stored energy is needed to feed the critical loads in the period between $t = 2$ and $t = 24$ h. During the second hour, the system is able to feed all the loads. Once the first two hours have elapsed, the system enters in resilience mode during 24 h and feeds only the critical loads. In the following hours, the system will store the generated energy in the hybrid ESS in order to satisfy the load requirement when generation power is not available. Notice that in the sample instants $t = 2$ to $t = 4$ the connection with the grid is interrupted. As can be seen, the generated energy will saturate the maximum level of energy stored in the batteries and the hydrogen tank. As there is not the possibility to exchange energy with the main grid, it is necessary to perform a generation curtailment.

In Fig. 7, from hour 1 to hour 3, the microgrid has connection with the grid being able to exchange energy with it. From hour 4 to 5, the system enters in survivability mode and has to cut some of the non-critical loads, because the LOH and SOC level are in their minimum value at hour 6, when the connection with grid is interrupted and the critical loads have to be supplied. From hour 5 onwards, the behavior is similar to case study of Node 1 (Fig. 6).

Fig. 8 is similar to Node 4, but in this case, it is not necessary to cut any non-critical load during the survivability period, the excess of power generation in hours 8 and 9 allows to feed all the loads.

In the scenario represented in Fig. 9, at the sample instants corresponding to $t = 16$ h and $t = 17$ h, while the system is in survivability mode, some non-critical loads have to be shut down because from that moment on the system will not be able to buy energy from the grid and in hour 30 the storage of the energy systems reaches its minimum

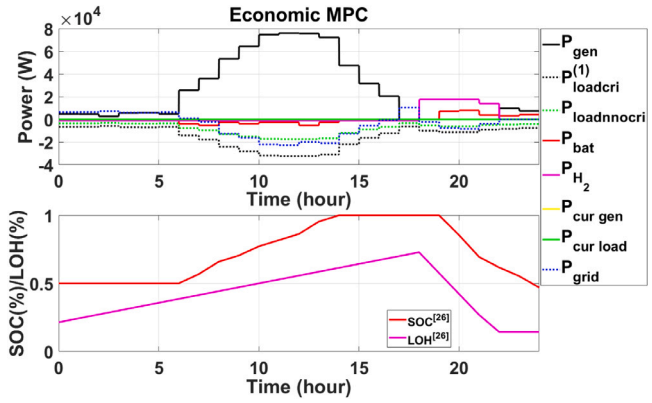

Fig. 11. Economic MPC.

value. If these non-critical loads were not cut off, the microgrid would not be able to fed the critical loads at the sample instant $t = 30$ h. Also, the system prioritizes the use of the battery during grid-connected mode, but when the power connection with the grid is lost, it starts to prioritize the use of hydrogen. This can be seen from hour 31 onwards.

In the corresponding scenario to node 24 (Fig. 10), the microgrid works for 23 h in grid connected mode, and from the 23rd to the 47th hour, the EMS faces a grid blackout during 24 h. During the first 23 h, the system purchases energy from the grid and uses it either to increase the energy stored in the hybrid ESS or to feed the loads. As can be seen at the sample instant $t = 18$ h, the EMS prioritizes the use of hydrogen to feed the loads rather buying energy. From the 23rd to the 47th hour, the process is similar to the represented one in Fig. 6 (Node 1): the algorithm calculates the optimal use of the hybrid ESS and the energy generated in order to accomplish the 24 resilience hours.

Once the SH = 24 scenarios have been carried out by the Resilience MPC control block, the Economic MPC block optimizes the microgrid by employing the aforementioned matrix, using the maximum of each column (maximum value for each hour) as the minimum LOH and SOC and returns the result shown in Fig. 11. In this case, there will be critical and non-critical loads during the whole span of the test. The energy balance established in (18) is achieved at hourly intervals. The system will now be able to buy energy from and sell it to the grid, and once the ESS storage constraints at a given instant are met, the system will then evaluate whether it is profitable to sell the excess of energy at that instant, or store more energy in the ESS and sell it at future instants. Similarly, if the system needs more ESS storage, it will buy energy from the grid.

Finally, Table 4 shows a comparison of the LOH and SOC obtained in each scenario of the Resilience MPC control block and the value obtained in the optimization carried out by the Economic MPC Control Block. Both the $LOH_{cri(s)}$ and $SOC_{cri(s)}$ are the most restrictive in all the scenarios of the resilience MPC in each hour, thus meeting the survivability and critical criteria in the Economic MPC. Furthermore, LOH_{min} and SOC_{min} are the values obtained in the Economic MPC in Fig. 11.

Table 4
Comparison between the minimum LOH and SOC obtained by multi-scenario and the LOH and SOC of the MPC.

Hour	$LOH_{cri(s)}$	LOH_{min}	$SOC_{cri(s)}$	SOC_{min}
1	24.29%	24.29%	50%	50%
2	27.14%	27.14%	50%	50%
3	30%	30%	50%	50%
4	32.86%	32.86%	50%	50%
5	35.71%	35.71%	50%	50%
6	38.57%	38.57%	50%	50%
7	41.43%	41.43%	56.82%	56.82%
8	44.29%	44.29%	65.94%	65.94%
9	47.14%	47.14%	70.5%	70.05%
10	50%	50%	77.2%	77.2%
11	52.86%	52.86%	81.76%	82.5%
12	55.71%	55.71%	86.32%	88.64%
13	58.57%	58.57%	95.44%	95.44%
14	61.43%	61.43%	100%	100%
15	64.29%	64.29%	100%	100%
16	67.14%	67.14%	100%	100%
17	70%	70%	100%	100%
18	72.29%	72.86%	100%	100%
19	57.51%	57.51%	100%	100%
20	42.16%	42.16%	85.41%	85.41%
21	26.82%	26.82%	62.91%	69.41%
22	14.3%	14.3%	53.44%	61.88%
23	14.3%	14.3%	47.1%	55.34%
24	14.3%	14.3%	46.93%	46.93%

4. Conclusions

This paper provides a detailed description of a new procedure based on a hybrid and stochastic MPC with which to optimize the day-ahead participation of a microgrid linked to critical services, which has been validated via numerical simulations. A hybrid ESS composed of batteries and hydrogen tanks, characterized by high power density and high energy density, was integrated in the microgrid studied. The proposed methodology guarantees the required resilience of the microgrid when it is needed by facilities and installations with critical loads, such as hospitals, military bases, research centers or transport stations.

The numerical results show that the proposed methodology guarantees the supply of electricity to the internal loads of the microgrids after a power outage event in the main power grid at any sample instant without reserving a specific level of stored energy, as has occurred previously in the existing literature. The control strategy developed makes it possible to maximize the capacity of each ESS. In order to improve the flexibility of the microgrid operation in the case of a transition from the grid-connected mode to the islanded mode, two levels of resilience are proposed: criticality and survivability.

The control problem was solved using MPC techniques involving a Mixed Integer Quadratic Programming (MIQP) formulation based on the optimization of a multi-scenario scheme. The use of MPC controllers makes it possible to integrate the behavior of the microgrid components through the use of a model. This feature allows the optimization of the setpoints given to each ESS by considering degradation issues and operation cost, thus improving their economic revenue and maximizing their lifetime. The formulation of the MPC algorithm within the MLD framework makes it possible to integrate optimization variables, such as working hours or switching states. The introduction of the multi-scenario criteria allows the minimum level of the SOC and LOH to be maximized without reserving a constant minimum level of stored energy in order to maintain the resilience criterion of the microgrid.

Several potential shortcomings have been detected during the research time dedicated to the development of this article. As only the pessimist scenario (see Ref. [18]) for the energy forecast is considered in the optimization of the critical scenarios, the algorithm should continuously evaluate if the stored energy can proportionate longer periods of survivability. This is one of the research lines which will be followed in future papers. It is also proposed the research line applied to interconnected microgrids to enhance the resilience of energy communities based on microgrids. Finally, as is well known, renewable energy microgrids have a schedule that is subject to the uncertainties contemplated in their predictive model. Although the proposed methodology is not focused on the prediction and forecast model, these uncertainties have to be taken into account. Apart from the minimum level of energy storage calculated by the proposed 'Resilience MPC Module', a band of stored energy reserve should also be added in order to consider the inaccuracies that result from applying the

prediction model carried out for the proposed optimization algorithm of the microgrid. Future developments of the current work may add these uncertainties to the algorithm, thus enhancing the proposed algorithm through the integration of Stochastic MPC techniques.

CRediT authorship contribution statement

Javier Tobajas: Conceptualization, Methodology, Software, Writing – original draft. **Felix Garcia-Torres:** Writing – original draft, Investigation, Conceptualization. **Pedro Roncero-Sánchez:** Writing – review & editing, Visualization. **Javier Vázquez:** Writing – review & editing, Visualization. **Ladjel Bellatreche:** Writing – review & editing. **Emilio Nieto:** Writing – review & editing.

Declaration of competing interest

The authors declare that they have no known competing financial interests or personal relationships that could have appeared to influence the work reported in this paper.

Acknowledgment

This work has been carried out with the financial support of the European Regional Development Fund (ERDF) under the Interreg SUDOE SOE3/P3/E0901 (Project IMPROVEMENT) program.

References

[1] Van den Broeck G, Stuyts J, Driesen J. A critical review of power quality standards and definitions applied to DC microgrids. Appl Energy 2018;229:281–8.
[2] Hussain A, Bui V-H, Kim H-M. Microgrids as a resilience resource and strategies used by microgrids for enhancing resilience. Appl Energy 2019;240:56–72.
[3] Adefarati T, Bansal R. Reliability, economic and environmental analysis of a microgrid system in the presence of renewable energy resources. Appl Energy 2019;236:1089–114.
[4] Bordons C, Garcia-Torres F, Ridao MA. Model predictive control of microgrids, vol. 358. Springer; 2020.
[5] Wu R, Sansavini G. Integrating reliability and resilience to support the transition from passive distribution grids to islanding microgrids. Appl Energy 2020;272:115254.
[6] Hossain E, Roy S, Mohammad N, Nawar N, Dipta DR. Metrics and enhancement strategies for grid resilience and reliability during natural disasters. Appl Energy 2021;290:116709.
[7] Mishra S, Anderson K, Miller B, Boyer K, Warren A. Microgrid resilience: A holistic approach for assessing threats, identifying vulnerabilities, and designing corresponding mitigation strategies. Appl Energy 2020;264:114726.
[8] Morato MM, Mendes PR, Normey-Rico JE, Bordons C. LPV-MPC fault-tolerant energy management strategy for renewable microgrids. Int J Electr Power Energy Syst 2020;117:105644.
[9] Morato MM, Regner DJ, Mendes PR, Normey-Rico JE, Bordons C. Fault analysis, detection and estimation for a microgrid via H2/H∞ LPV observers. Int J Electr Power Energy Syst 2019;105:823–45.
[10] Prodan I, Zio E, Stoican F. Fault tolerant predictive control design for reliable microgrid energy management under uncertainties. Energy 2015;91:20–34.
[11] Roslan M, Hannan M, Jern Ker P, Begum R, Indra Mahlia T, Dong Z. Scheduling controller for microgrids energy management system using optimization algorithm in achieving cost saving and emission reduction. Appl Energy 2021;292:116883.
[12] Cattaneo A, Madathil SC, Backhaus S. Integration of optimal operational dispatch and controller determined dynamics for microgrid survivability. Appl Energy 2018;230:1685–96.
[13] Du W, Lasseter RH, Khalsa AS. Survivability of autonomous microgrid during overload events. IEEE Trans Smart Grid 2018;10(4):3515–24.
[14] Khodaei A. Resiliency-oriented microgrid optimal scheduling. IEEE Trans Smart Grid 2014;5(4):1584–91.
[15] Hussain A, Bui V-H, Kim H-M. Resilience-oriented optimal operation of networked hybrid microgrids. IEEE Trans Smart Grid 2017;10(1):204–15.
[16] Zakernezhad H, Nazar MS, Shafie-khah M, Catalão JP. Optimal resilient operation of multi-carrier energy systems in electricity markets considering distributed energy resource aggregators. Appl Energy 2021;299:117271.
[17] Garcia-Torres F, Bordons C. Optimal economical schedule of hydrogen-based microgrids with hybrid storage using model predictive control. IEEE Trans Ind Electron 2015;62(8):5195–207.
[18] Garcia-Torres F, Bordons C, Tobajas J, Real-Calvo R, Santiago Chiquero I, Grieu S. Stochastic optimization of microgrids with hybrid energy storage systems for grid flexibility services considering energy forecast uncertainties. IEEE Trans Power Syst 2021;1.
[19] Garcia-Torres F, Valverde L, Bordons C. Optimal load sharing of hydrogen-based microgrids with hybrid storage using model-predictive control. IEEE Trans Ind Electron 2016;63(8):4919–28.
[20] Alhasnawi BN, Jasim BH, Sedhom BE. Distributed secondary consensus fault tolerant control method for voltage and frequency restoration and power sharing control in multi-agent microgrid. Int J Electr Power Energy Syst 2021;133:107251.
[21] Khederzadeh M, Zandi S. Enhancement of distribution system restoration capability in single/multiple faults by using microgrids as a resiliency resource. IEEE Syst J 2019;13(2):1796–803.
[22] Aluisio B, Dicorato M, Forte G, Trovato M. An optimization procedure for microgrid day-ahead operation in the presence of CHP facilities. Sustain Energy Grids Netw 2017;11:34–45.
[23] Parisio A, Rikos E, Glielmo L. A model predictive control approach to microgrid operation optimization. IEEE Trans Control Syst Technol 2014;22(5):1813–27.
[24] Samimi A, Nikzad M, Siano P. Scenario-based stochastic framework for coupled active and reactive power market in smart distribution systems with demand response programs. Renew Energy 2017;109:22–40.
[25] Parisio A, Rikos E, Glielmo L. Stochastic model predictive control for economic/environmental operation management of microgrids: An experimental case study. J Process Control 2016;43:24–37.
[26] Bazmohammadi N, Tahsiri A, Anvari-Moghaddam A, Guerrero JM. Stochastic predictive control of multi-microgrid systems. IEEE Trans Ind Appl 2019;55(5):5311–9.
[27] Velarde P, Valverde L, Maestre JM, Ocampo-Martínez C, Bordons C. On the comparison of stochastic model predictive control strategies applied to a hydrogen-based microgrid. J Power Sources 2017;343:161–73.
[28] Barelli L, Bidini G, Cherubini P, Micangeli A, Pelosi D, Tacconelli C. How hybridization of energy storage technologies can provide additional flexibility and competitiveness to microgrids in the context of developing countries. Energies 2019;12(16):3138.
[29] Tan X, Li Q, Wang H. Advances and trends of energy storage technology in microgrid. Int J Electr Power Energy Syst 2013;44(1):179–91.
[30] Valverde L, Rosa F, Bordons C. Design, planning and management of a hydrogen-based microgrid. IEEE Trans Ind Inf 2013;9(3):1398–404.
[31] Ju C, Wang P, Goel L, Xu Y. A two-layer energy management system for microgrids with hybrid energy storage considering degradation costs. IEEE Trans Smart Grid 2018;9(6):6047–57.
[32] Koohi-Fayegh S, Rosen MA. A review of energy storage types, applications and recent developments. J Energy Storage 2020;27:101047.
[33] Bemporad A, Morari M. Control of systems integrating logic, dynamics, and constraints. Automatica 1999;35(3):407–27.